

## LIDAR MEASUREMENTS OF MIDDLE AND LOWER ATMOSPHERE PROPERTIES DURING THE LADIMAS CAMPAIGN

C. R. Philbrick, D. B. Lysak, T. D. Stevens, P. A. T. Haris and Y.-C. Rau

*The Pennsylvania State University  
Department of Electrical Engineering and Applied Research Laboratory  
University Park, PA 16802*

### ABSTRACT

The results of the Latitudinal Distribution of Middle Atmosphere Structure (LADIMAS) experiment have provided a unique data set to improve our understanding of the middle atmosphere properties. The project included coordinated ship-board measurements between 70N to 65S and measurements at the Andoya rocket range to study the structure, dynamics and chemistry of the atmosphere. Results on dynamical processes, such as gravity waves, as well as, the formation of the layers of meteoric ion and neutral species, have been obtained using lidars, digisonde, microwave radiometer, and spectrometers. The cooperative study of the atmosphere was undertaken by researchers from several laboratories, including Penn State University, University Bonn, University Wuppertal, Lowell University, and others. Instruments were assembled aboard the German research vessel RV *Polarstern* while this vessel was sailing from the Arctic to the Antarctic between October 8, 1991 and January 2, 1992. An overview of the results from the PSU lidar investigation is presented here.

**Keywords:** Lidar, middle atmosphere structure, laser remote sensing, Pinatubo volcano aerosols, shipboard measurements

### 1. SUMMARY

As part of the Latitudinal Distribution of Middle Atmospheric Structure (LADIMAS) program (Ref. 1) on the German research ship RV *Polarstern*, measurements were made by the experiments listed in Table I during the voyage indicated in Figure 1. Data collected over this range of latitudes included lidar profiles of density and temperature from altitudes of 1 to 80 km (Ref. 2), profiles of minor meteoric Na and Fe species from 80 to 110 km, microwave-radiometer water vapor profiles from 40 to 80 km (Ref. 3), digital ionosonde profiles of electron/ion density from 85 to 150 km, measurements of mesospheric ozone variation in the layer from 90 to 95 km with an infrared spectrometer, profiles of aerosols from the surface to 40 km (Refs. 4, 5, 6, 7), tropospheric water vapor profiles (Ref. 8) and temperature measurements at 86 km with an OH spectrometer. Rawinsonde balloon-borne meteorological instruments were released from the ship during the campaign transit over the latitude range.

A two-color Rayleigh/Raman lidar has been developed to study the properties of the middle and lower atmosphere. The LAMP (Lidar Atmospheric Measurements Program) lidar profiler was

Table I LADIMAS Experiments

| Instrument                 | Measurements  | Organization   |
|----------------------------|---|--|
| Iron Resonance Lidar       | atmospheric dynamics from 80 to 110 km  | Bonn University  |
| Sodium Resonance Lidar     | atmospheric dynamics 80-110 km profiles   | Bonn University  |
| LAMP Lidar                 | molecular, particle, and Raman scattering for profiles of temperature, density and H <sub>2</sub> O from 200 m to 80 km | Penn State University  |
| Microwave Radiometer       | 22 GHz emission, H <sub>2</sub> O molecules for H <sub>2</sub> O profiles from 40 to 80 km                              | Penn State University  |
| Digisonde                  | electron/ion density  | Penn State University and University of Massachusetts (Lowell) |
| IR Spectrometer            | infrared emission by OH radicals for temperature measurement from 82 to 92 km to determine altitude of mesopause        | Wuppertal University   |
| Near Infrared Spectrometer | temperature from 88 to 95 km  | Saskatchewan University  |

placed in service at Penn State University during the summer of 1991. The LAMP lidar uses two wavelengths in the upward propagating beam and up to eight detectors in the receiver. The instrument is arranged in a coaxial configuration, which permits useful measurements in the near field, as well as in the far field, see Figure 2. The detector system uses a mechanical shutter to block the high intensity, low altitude signal, from the high altitude detectors until the beam has reached an altitude of typically 15 to 20 km. The Nd:YAG laser beam is passed through a doubling crystal and a mixing crystal to produce a 532 and a 355 nm beam. The low altitude backscatter signals of the visible and ultraviolet beams are detected as analog signals and digitized at 10 MSps to provide 15 meter resolution from the surface to 25 km. The high altitude signals, obtained by photon counting techniques, are accumulated into 500 nanosecond range bins to provide 75 meter resolution, from 20 to 80 km. The detector also contains low altitude photon counting channels which measure the first Stokes vibrational Raman signals of the N<sub>2</sub> at 607 nm and the H<sub>2</sub>O at 660 nm. We have investigated the possibility of measuring the temperature profile in the turbid lower atmosphere using the N<sub>2</sub> vibrational Raman signal. However, this approach has proven to be quite limited due to the

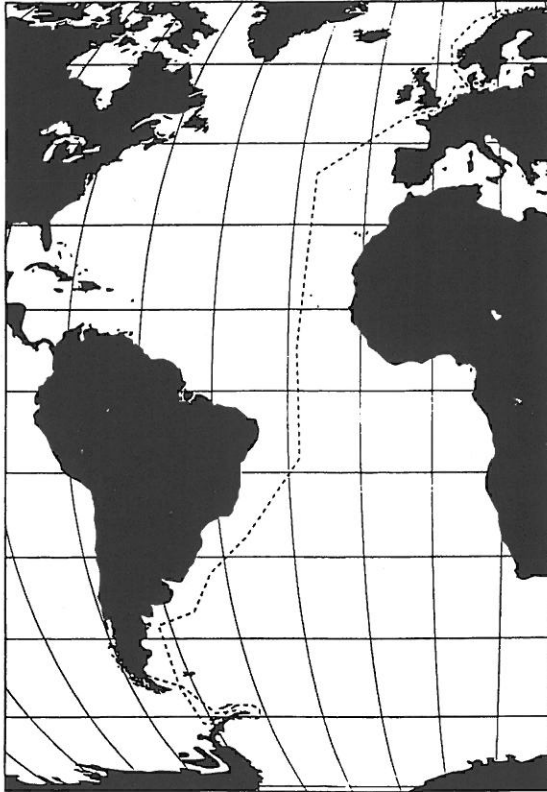


Figure 1. The voyage of the RV *Polarstern*, October 1991 - January 1992.

accuracy with which the extinction can be determined when cloud layers are present. Measurements of the rotational Raman backscatter are being investigated as the appropriate way to measure the temperature profiles in the presence of clouds and in the boundary layer. The LADIMAS measurements have allowed the preparation of a map of the Pinatubo volcano aerosol distribution and an investigation of the latitudinal variation in the density and temperature structure of the middle atmosphere. Studies of the distribution of tropospheric water vapor and tropospheric aerosols, and an investigation of the optical scattering properties of the atmosphere have also been carried out using the results.

## 2. MEASUREMENTS

The LAMP (Lidar Atmospheric Measurements Program) lidar instrument is an advanced laser remote measurement sensor which has been built-up during 1990-1991. The design follows the progressive development of our two previous lidar designs [Refs. 9, 10]. This instrument extends the measurement range downward to cover the troposphere as well as the stratosphere and mesosphere, using the molecular and Raman backscatter signals at several wavelengths to determine the profile distributions of density, temperature, extinction, particle backscatter, and water vapor concentration. The instrument uses a high power Nd:YAG laser with an output of 1.5 J/pulse at 20 Hz. The fundamental wavelength is doubled to obtain 600 mJ pulses at 532 nm and mixed to obtain 225 mJ pulses at 355 nm or doubled again to produce 80 mJ pulses at 266 nm. The transmitter, receiver, detector, and data system combination have been integrated into a standard shipping container, which serves as a field laboratory. The primary receiver is a 42 cm diameter

Cassegrainian telescope. Measurements of the back-scatter radiation are typically made simultaneously at the laser output wavelengths of 532 and 355 nm, with several different detectors in order to cover the dynamic range and to obtain information at selected Raman shifted wavelengths. Figure 3 shows two examples of the raw lidar signal, corrected for  $1/R^2$  dependence, which are typical of the signals measured on several of the data channels. The figures show the signal from boundary layer aerosols, tropospheric clouds, high cirrus clouds and stratospheric aerosol layers. The low altitude channels for 532 and 355 nm receive about 5% of the collected signal intensity and the measurements are made in analog mode with an A/D converter at 10 MHz (15 meter altitude steps) with 12 bit resolution. The high altitude channels are mechanically shuttered below 15 km to prevent the PMT's from being saturated by the large signal received from there. The high altitude channels and the Raman channels for  $N_2$ , at 607 nm, and for  $H_2O$ , at 660 nm, use photon counting detectors, with range bins of 500 nanoseconds (75 meter altitude steps). A smaller telescope, 20 cm diameter, was used for independent bistatic measurements, usually at the 532 nm wavelength, to provide an independent overlap of the altitude region 10 to 30 km. In Figure 4, the profiles of the low and high altitude channels have been overlapped to provide continuous profiles from 200 meters to 80 km. The back-scatter and extinction associated with the stratospheric aerosols, clouds and the boundary layer can be readily observed in the profiles at these two wavelengths. Notice that the scattering ratio of the 532 nm compared to the 355 nm changes significantly with the changing size of the particle scatterers. When the stratospheric aerosol scattering intensities are compared to those for the tropospheric clouds, the change in extinction and back-scatter cross-section with particle size is obvious. One of the more important observations from the LADIMAS results is the significance of the two-wavelength lidar approach in defining the particle scattering layers of the atmosphere, particularly the lower stratospheric aerosol and particle layer. The boundary where the high altitude signal, above about 30 km, can be analyzed to provide density and temperature profiles can be identified using the two-wavelength approach.

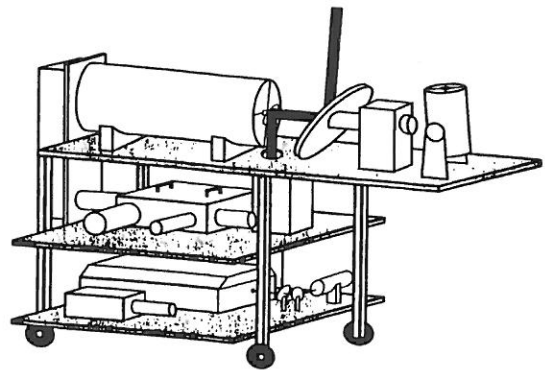


Figure 2. A diagram of the LAMP lidar shows the laser on the bottom of the table, the detector on the middle shelf, and the receiving telescope at the top with the beam steering mirror.

The initial data of LADIMAS, for the LAMP instrument, were gathered at Andoya Rocket Range, Norway. On the leg between Tromsø, Norway, and Bremerhaven, Germany, the operational testing of the LAMP lidar instrument on the ship was completed.

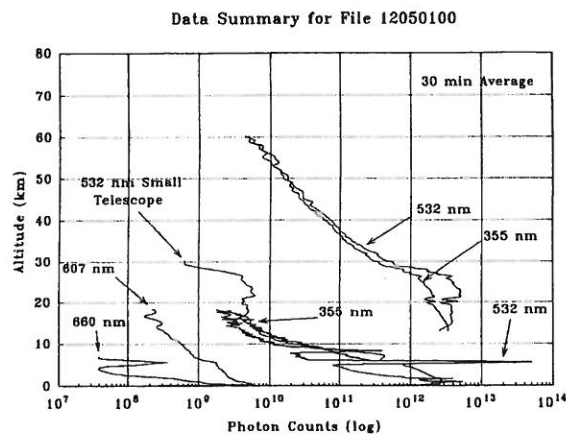
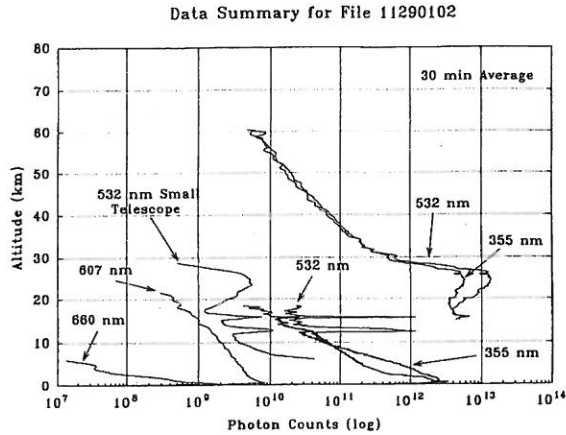


Figure 3. Examples of the raw signals, corrected for  $1/R^2$ , for the low and high altitude channels, signals from the small telescope, and Raman channels are shown.

Measurements were made on each clear night, and on some occasions, the measurements were made below and into the clouds. The measurements included high and low altitude channels for the 532 and 355 nm wavelengths, Raman shifted  $N_2$  at 607 nm, Raman shifted  $H_2O$  at 660 nm, and 532 nm measurements from a second telescope simultaneously recorded. The variations in the profile, see Figures 3 and 4, near 25 km are due to particle scattering. One of the more striking features observed by the LADIMAS instruments is the lower stratospheric aerosol and particle layers. The high altitude signal, above about 30 km, can be easily analyzed to provide density and temperature profiles (Ref. 11). The two-color approach (Refs. 9, 10) allows the detection and separation of the molecular and particle components. Note that the particle scattering relative intensity is much stronger for the 532 than for the 355 signals. The cross-section for the molecular scatterers is much larger at 355 nm, while the particle cross-section may not differ significantly between the two wavelengths (for example, see Ref 12). Figure 5 shows the measured signals of the 355 and 532 nm channels, together with the profiles of the aerosol scattering ratio to the molecular scattering, in this case, unity has been subtracted. The extinction due to the strong scattering layers is obvious in the profiles.

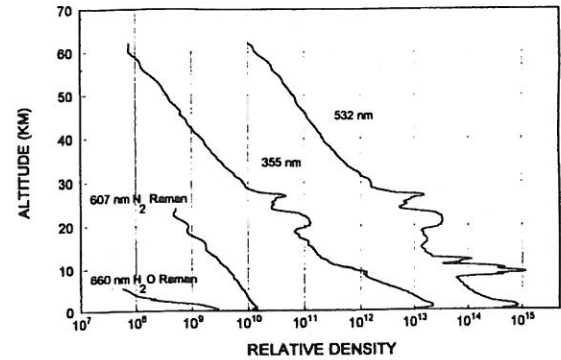


Figure 4. Examples of the continuous profiles of the data are shown. The slope change below 1 km is due to telescope focus and geometrical factors.

Figure 6 shows the latitudinal plot of the scattering ratio for the 355 and 532 nm wavelengths. The strong variations in the scattering ratio as a function of latitude are a result of the Pinatubo volcano eruption which injected large quantities of aerosols at stratospheric heights (see Ref. 13). The two color lidar shows a large difference in relative back-scatter intensity from the stratospheric aerosols, primarily due to the smaller molecular scatter component at 532 nm, but also due to the fact that the stratospheric aerosols are sufficiently small that the wavelength dependence of scattering is significant. The results indicate that the particle size is comparable to the wavelengths of the lidar. When the molecular scattering component is removed and the particle scattering is examined, the size distribution of stratospheric aerosols is found to be remarkable stable, exhibiting a uniform ratio in the scattering intensity for the two wavelengths, see Figure 5. The measurements from the lidar on board the *Polarstern* have been compared with the aerosol extinction measurements of the limb-looking SAGE II instrument (Ref. 14). The comparison between the extinction curves is made at the 1020 nm wavelength. The SAGE II instrument tangent point in the limb crossed near the shipboard lidar on several occasions. One example of the extinction profile comparisons is shown in Figure 7.

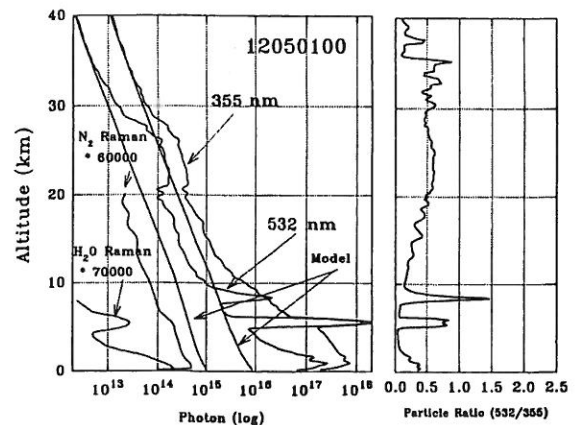


Figure 5. The profiles of the particle backscatter intensity at the two wavelengths are compared by using a reference model for the molecular scattering component tied to the profile at 40 km.

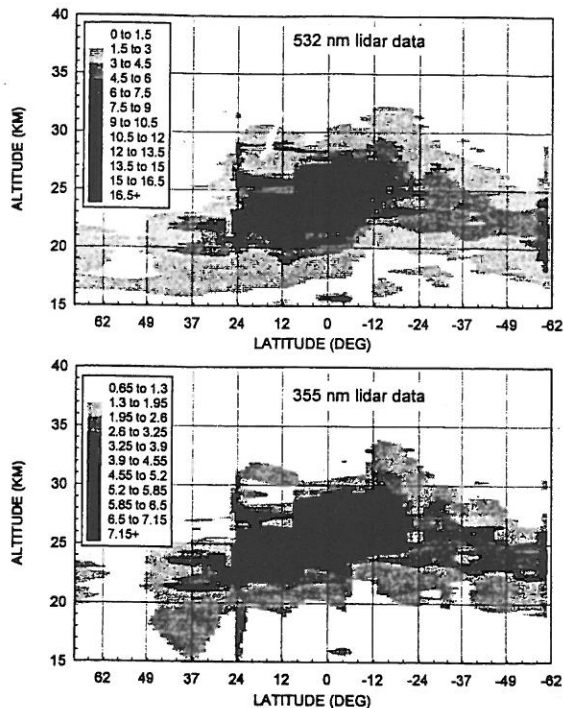


Figure 6. The latitudinal profile of the 532 and 355 nm signals show the stratospheric aerosol layers formed by the Pinatubo volcano. The results were primarily obtained between mid-November and the end of December 1991, about five months after the volcano eruption.

The LAMP lidar was operated at the Andoya Rocket Range, Norway, during September/October 1991. Measurements which allow the comparisons of the lidar and rocket data were carried out. Figure 8 shows a comparison of lidar and rocket measurements made on 4 October 1991. A large comparison study in 1986 (Refs. 9, 10) had shown good agreement between lidar and meteorological rockets carrying passive spheres and datasondes. This experiment provided two additional data comparisons, bringing the total to more than twenty investigations. The average values of the measurements made by the lidar were grouped into bins by latitude and season to make comparisons with standard models (see Ref. 2). Figure 9 shows a comparison of one of these average profiles compared with the CIRA 1986 and USSA 1976 models. The summary of the study is shown in Figure 10. The density and temperature variations measured by the lidar are summarized relative to the models. In general, we find the average lidar results to be in surprisingly good agreement with the CIRA model.

At tropospheric altitudes, the Raman  $N_2$  profile together with the two-color back-scatter should allow the separation of the extinction, back-scatter due to particles and the molecular back-scatter signals. The advantage in using the Raman signals in the lower atmosphere is clear from the profiles shown above. Figure 11 shows a representation of the spectral signatures which would be expected from the back-scatter due to the 532 nm laser radiation in an atmospheric volume (see Ref. 15 and 16). The laser is injection seeded to give a line-width of about 80 MHz and thus the particle back-scatter is of that spectral width, while the molecular peaks are broadened by the thermal Doppler spreading. The vibrational Raman scattering peaks are shown for  $O_2$ ,  $N_2$  and  $H_2O$ . Each of the peaks is also broadened at their

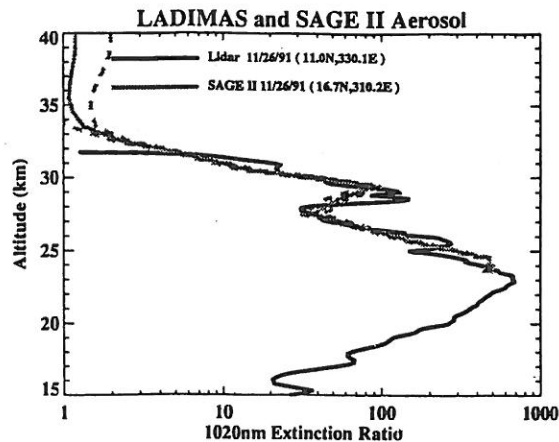


Figure 7. Extinction profiles from the LAMP lidar on the Polarstern and SAGE II satellite limb retrieval on 26 November 1991 (provided by Veiga and McCormick, see Ref. 14).

base due to the rotational state distribution around each vibrational state. Only the first Stokes vibrational states are indicated. The figure shows the large cross-section differences between the processes involved. The Raman  $H_2O$  signal measured as a ratio to the Raman  $N_2$  signal provides an accurate profile of the water vapor concentration, since the  $N_2$  fraction of the atmospheric profile is known, and the atmospheric profile can be obtained from pressure or temperature profiles combined with surface values. The error caused by the extinction differences between the backscatter wavelengths is small (few percent) and can be corrected using the multiple wavelengths. Figure 12 shows the profiles of the water vapor concentration compared with rawinsonde balloon data. The prior work of Melfi (Ref. 17) has shown the power of the Raman technique for obtaining water vapor measurements. The results gathered here have provided a data base from which a critical analysis of the technique can be made.

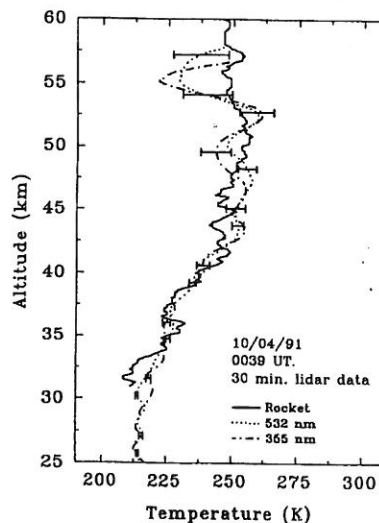


Figure 8. Results from simultaneous measurement by lidar and meteorological rocket at Andoya Rocket Range, Norway on 4 October 1991.

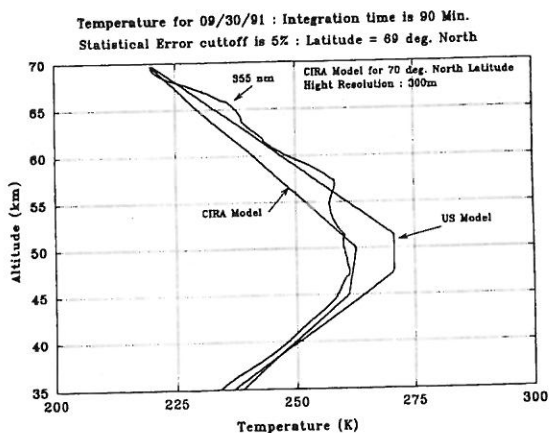


Figure 9. Comparison of the average lidar temperature results with the CIRA 1988 and USSA 1976 in one bin of latitude and season.

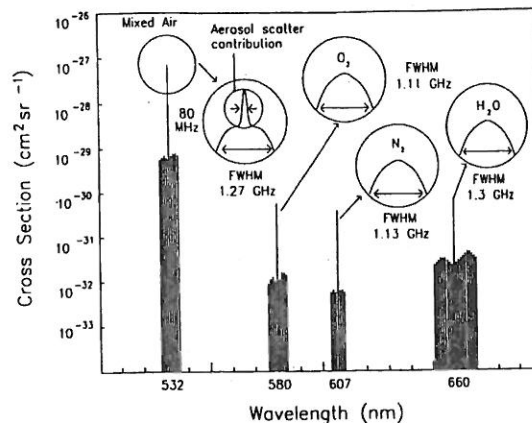


Figure 11. Descriptive representation of the vibrational and rotational Raman signals expected for radiation of an atmospheric volume with 532 nm laser.

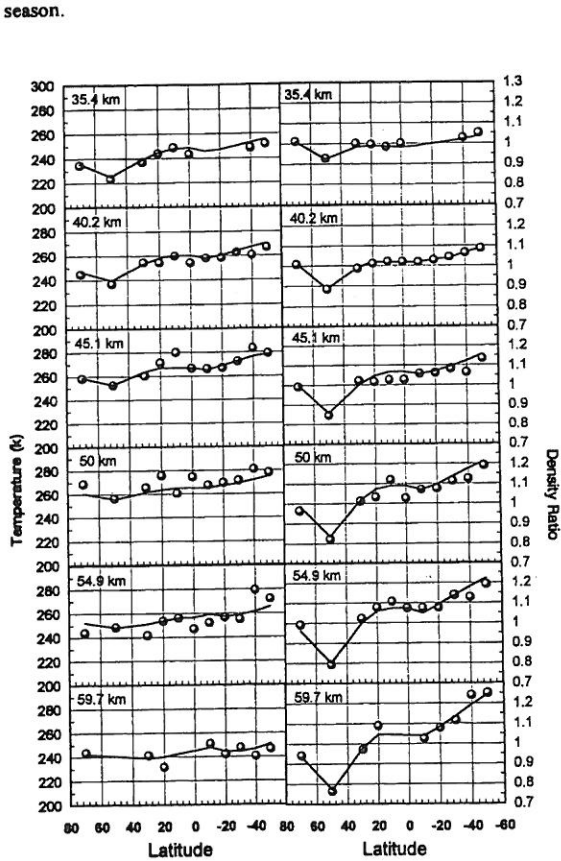


Figure 10. Summary of the lidar average results for density and temperature variations compared to the CIRA model. The lidar average values for each bin of latitude, altitude and season are shown as circles and the line is the CIRA model. The density measurement and CIRA ratios are relative to the constant model of the USSA 76.

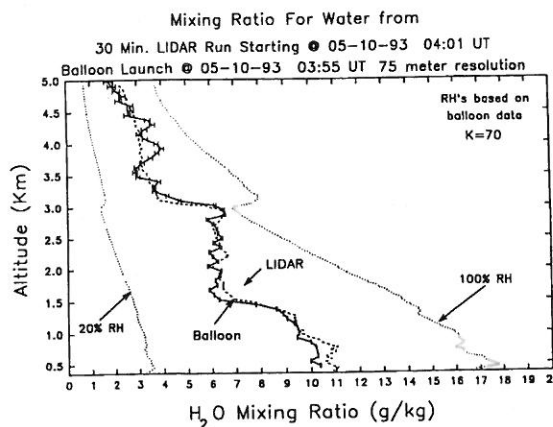


Figure 12. Example of the water vapor concentration obtained from the Raman lidar signals, with one sigma error shown, compared with a rawinsonde balloon profile.

The LAMP lidar activities are being extended in several ways to make investigations of the properties of the atmosphere. The work in progress extends the measurements into daylight hours with improvements in detector filters and by making tropospheric measurements in the solar blind portion of the spectrum. The development of the LARS lidar instrument provides capability to volume scan the backscatter intensity at several wavelengths with polarization information (Ref. 18). We have planned and simulated the performance of a direct detection wind measuring lidar which make use of a new approach to Doppler lidar measurements (Ref. 19). The chance to obtain the concentrated set of measurements on the RV *Polarstern* over such a wide range of latitude was a special opportunity. The work in progress on those results will produce several additional papers during the coming year. Improved measurements of the properties of the atmosphere are required for meteorological forecasting, operational test support and for studies of the global environment. The long term goal of these efforts is to develop a lidar instrument which can provide routine measurements of the atmospheric properties.

## ACKNOWLEDGEMENTS

The preparation of the LAMP instrument has been supported by PSU/ARL project initiation funds, PSU College of Engineering, the Navy's Environmental Systems Program Office (SPAWAR PMW-165), and the National Science Foundation's CEDAR (Coupling Energetics and Dynamics of Atmospheric Regions) Program. The measurements on the RV *Polarstern* were made possible by invitation of the Alfred-Wegener-Institut which is gratefully acknowledged. The efforts of Professors O. Schrems and U. von Zahn in organizing the voyage are appreciated. The many years of collaborative efforts with Professors U. von Zahn and D. Offermann made these investigations possible. The efforts of D. E. Upshaw, T. W. Collins, D. W. Machuga, S. Maruvada, S. McKinley, G. Evanisko and G. Pancoast have contributed much to the success of this project.

## REFERENCES

1. Philbrick, C. R., D. B. Lysak, T. D. Stevens, P. A. T. Haris and Y.-C. Rau, "Atmospheric Measurements Using the LAMP Lidar during the LADIMAS Campaign," 16th International Laser Radar Conference, NASA Publication 3158, 651-654, 1992.
2. Haris, P. A. T., T. D. Stevens, S. Maruvada and C. R. Philbrick, "Latitude Variation of Middle Atmosphere Temperatures," accepted for publication in *Advances in Space Research*, 1994.
3. Croskey, C. L., C. R. Philbrick, J. P. Martone, T. D. Stevens, P. A. T. Haris, J. J. Olivero, S. E. Puliafito and S. C. McKinley, "A Comparison of Microwave Radiometer, Lidar, and Meteorological Balloon Observations of Water Vapor During the LADIMAS Campaign," Proceedings of the IEEE Topical Symposium on Combined Optical-Microwave Earth and Atmosphere Sensing, 203-206, 1993.
4. Stevens, T. D., P. A. Haris, Y.-C. Rau and C. R. Philbrick, "Latitudinal Lidar Mapping of Stratospheric Particle Layers," accepted for publication in *Advances in Space Research*, 1994.
5. Maruvada, S., Y.-C. Rau, G. R. Evanisko and C. R. Philbrick, "Laser Scattering in Clouds," Proceedings of the IEEE Topical Symposium on Combined Optical-Microwave Earth and Atmosphere Sensing, 215-219, 1993.
6. Philbrick, C. R., D. B. Lysak and Y.-C. Rau, "Lidar Measurements of Aerosol Scattering in the Troposphere and Stratosphere" Proceedings of the IEEE Topical Symposium on Combined Optical-Microwave Earth and Atmosphere Sensing, 107-110, 1993.
7. Stevens, T. D., S. Maruvada, T. J. Kane and C. R. Philbrick, "Lidar Observations of Mt. Pinatubo Aerosols: Effects on the Global Radiation Budget," Proceedings of the OSA Sixth Topical Meeting on Optical Remote Sensing of the Atmosphere, 5, 313-316, 1993.
8. McKinley, S. C., and C. R. Philbrick, "Tropospheric Water Vapor Concentrations Measured by a Penn State/ARL Lidar," Proceedings of the IEEE Topical Symposium on Combined Optical-Microwave Earth and Atmosphere Sensing, 185-188, 1993.
9. Philbrick, C. R., "Lidar Profiles of Atmospheric Structure Properties," *Earth and Atmospheric Remote Sensing, SPIE Vol. 1492*, 76-84, 1991.
10. Philbrick, C. R., et al., "Measurements of the High Latitude Middle Atmosphere Dynamic Structure Using Lidar, AFGL-TR-87-0053, Environmental Research Papers, No. 967, 1987.
11. Chanin, M.L. and A. Hauchecorne, "Lidar Observations of Gravity and Tidal Waves in the Middle Atmosphere," *J. Geophys. Res.*, 86, 9715, 1981.
12. Carswell, A.I., "Lidar Remote Sensing of Atmospheric Aerosols," *SPIE Vol. 1312*, 206-220, 1990.
13. McCormick, M.P., T.J. Swisler, W.P. Chu, and W.H. Fuller, Jr., "Post Volcanic Stratospheric Aerosol Decay as Measured by Lidar," *J. Atmos. Sci.*, 35, 1296-1303, 1978.
14. Trepte, C. R., R. E. Veiga and M. P. McCormick, "The Poleward Dispersal of Mount Pinatubo Volcanic Aerosol," *J. Geophys. Res.* 98, 18563-18573, 1993.
15. Measures, R. M., Laser Remote Sensing, Krieger Publishing, Malabar, FL, 108, 1992.
16. Inaba, H. and T. Kobayasi, "Laser-Raman Radar," *Optoelectronics*, 4, 101-123, 1972.
17. Melfi, S. H., J. D. Lawrence Jr. and M. P. McCormick, "Observation of Raman Scattering by Water Vapor in the Atmosphere," *Appl. Phys. Lett.*, 15, 295-297, 1969.
18. Rajan, S., G. R. Evanisko, T. J. Kane and C. R. Philbrick, "Aerosol Mapping of the Atmosphere Using a Multiple Wavelength Polarization Lidar," Proceedings of the IEEE Topical Symposium on Combined Optical-Microwave Earth and Atmosphere Sensing, 111-114, 1993.
19. Machuga, D. W., T. J. Kane and C. R. Philbrick, "A Direct Doppler Detection Lidar System for Atmospheric Winds," Proceedings of the IEEE Topical Symposium on Combined Optical-Microwave Earth and Atmosphere Sensing, 4-7, 1993.